Longitudinal impedance measurements and simulations for the crystal collimator in HL-LHC

D. Quartullo, N. Biancacci, F. Giordano, I. Lamas Garcia, M. Migliorati, A. Mostacci, S. Redaelli, B. Salvant, L. Teofili

Introduction

- The goniometers are crystal-based primary collimators installed in the LHC.
  - They use the channelling process in bent crystals to steer halo particles efficiently onto downstream collimators.

- Crystal collimation uses 4 mm-long silicon crystals that need to be approached very close to the high-intensity circulating beams.
  - This poses obvious concerns for machine impedance.

- The electromagnetic characterization of the goniometer is essential prior to its usage with high-intensity beams.
  - We want to prevent possible beam-induced instabilities and/or damage of the device components from excessive RF-heating.

- This talk focuses on the longitudinal impedance of the goniometer.
  - This impedance is also used to estimate the power-losses inside the device for different types of LHC and HL-LHC beams.

- Electromagnetic simulations are performed on a realistic model.
  - Care is taken to characterize the materials of each relevant sub-component.

- Numerical results are then compared with dedicated RF measurements.

Previous presentations

1. D. Quartullo and M. Migliorati, “UA9 goniometer longitudinal impedance studies." CERN Impedance Meeting, 10/05/2019.

2. D. Quartullo et al., “New RF measurements to characterize the longitudinal impedance of the LHC UA9 goniometer." 33th IWG Meeting, 27/06/2029.

3. D. Quartullo et al., “Analysis of the new RF measurements to characterize the longitudinal impedance of the LHC goniometer." CERN Impedance Meeting, 12/07/2019.

4. D. Quartullo et al., “Characterization of the longitudinal impedance of the LHC UA9 goniometer through RF measurements and simulations.“ 118th CERN ColUSM Meeting and 34th IWG Meeting, 02/08/2019.

5. D. Quartullo et al., “Updates on longitudinal impedance studies for the LHC goniometer." CERN Impedance Meeting, 13/12/2019.

6. D. Quartullo et al., “Updates on the longitudinal impedance of the LHC V2 goniometer.“ 127th CERN ColUSM Meeting, 29/05/2020.

7. D. Quartullo et al., “Longitudinal impedance simulations for LHC crystal goniometers and next steps discussion”, 41th IWG Meeting, 12/06/2020.

Contents

Detailed models of the goniometer (1/2)

- Currently, four goniometers are installed in the LHC.
  - Each ring contains one horizontal goniometer and one vertical goniometer.

Current goniometers in the LHC

Functional type	Position in the LHC	Design type	Design version	Installation year
TCPCH	A4L7.B1	ST	V1	2015
TCPCV	A6L7.B1	QM	V1	2015
TCPCH	A5R7.B2	ST	V2	2018
TCPCV	A6R7.B2	QM	V2	2017

- Both configurations share the same external structure which
  - guides and positions the goniometer on its dedicated support;
  - hosts the connection of the electronic systems (motorizations, switches, etc);
  - is able to adjust, on the three axes, the entire assembly and align it against the other LHC elements;
  - allows thermal expansion during bake-out and minimizes the positional displacement during cooling.

Horizontal goniometer and external structure

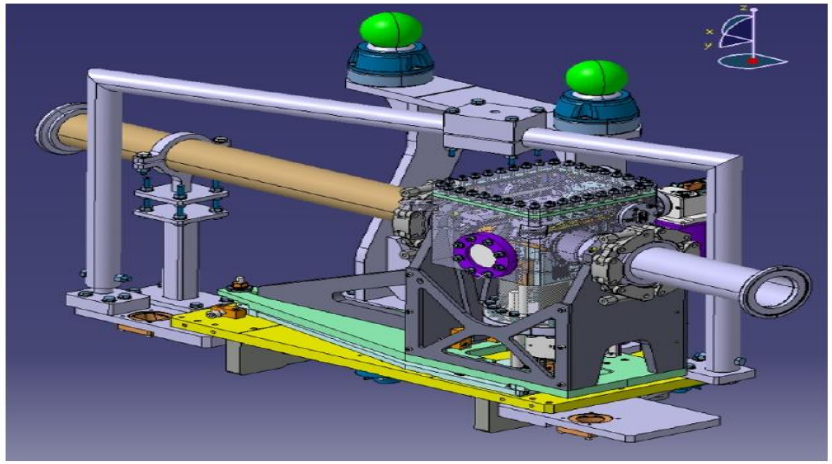

Vertical goniometer and external structure

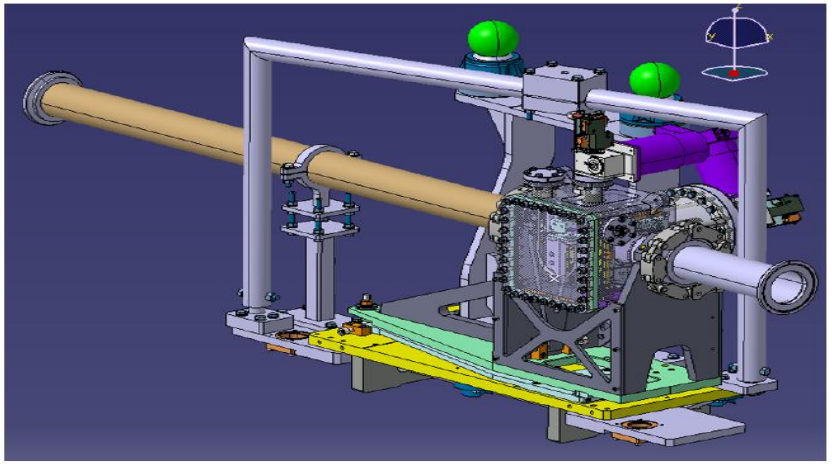

Detailed models of the goniometer (2/2)

- The crystal can be retracted and the auxiliary beam pipe can be parked in.
  - Standard operational position of the goniometer for LHC proton beams.
  - The device is completely transparent for the beam.
    - The RF contacts lead to airgaps with negligible impedances (studies by A. Danisi, 2014).

- With ion beams, the replacement chamber is retracted and the crystal is parked in for particle channelling.

- The linear stage and the holder support best allow the core functionalities of the goniometer.
  - They form a high precision system able to control both position and orientation of the crystal.

Cross sections of the V2 goniometer model (auxiliary beam-pipe parked in and crystal retracted)

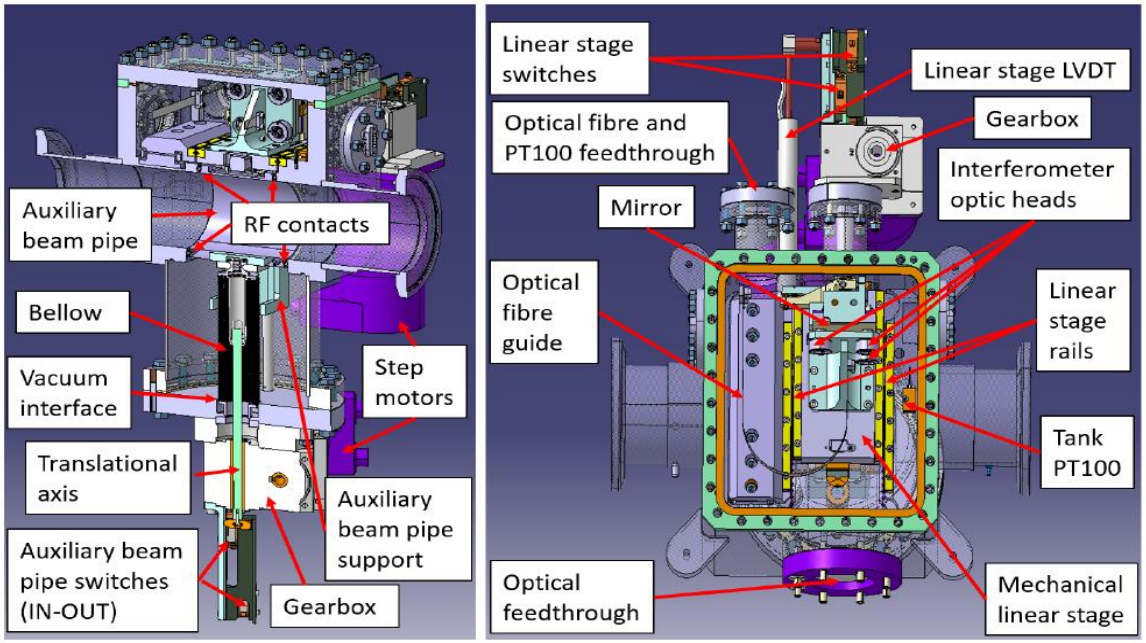

Linear stage (up), holder support, holder and crystal (bottom)

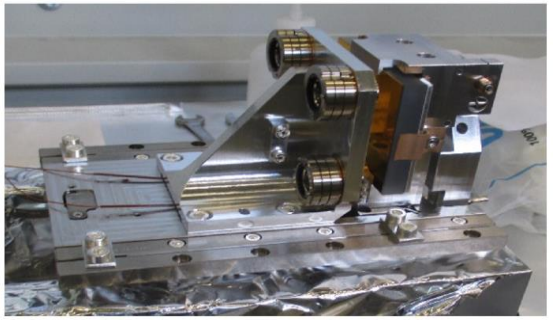

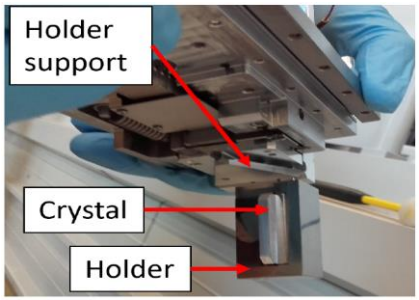

Contents

Model used in CST simulations

- The CAD model of the V2 goniometer was imported into CST.
- The external components which didn't influence the EM fields were removed.
- Apart from the two bellows, which couldn't be properly meshed and therefore were simplified as cylinders, all the other internal components were not modified.
  - The obtained model is reliable.
    - Previous studies show that internal simplifications must be done very carefully.
  - The obtained model leads to quite computationally expensive simulations due to the complexity of the internal structure of the goniometer.

Views of the V2 model used in simulations (dimensions in mm)

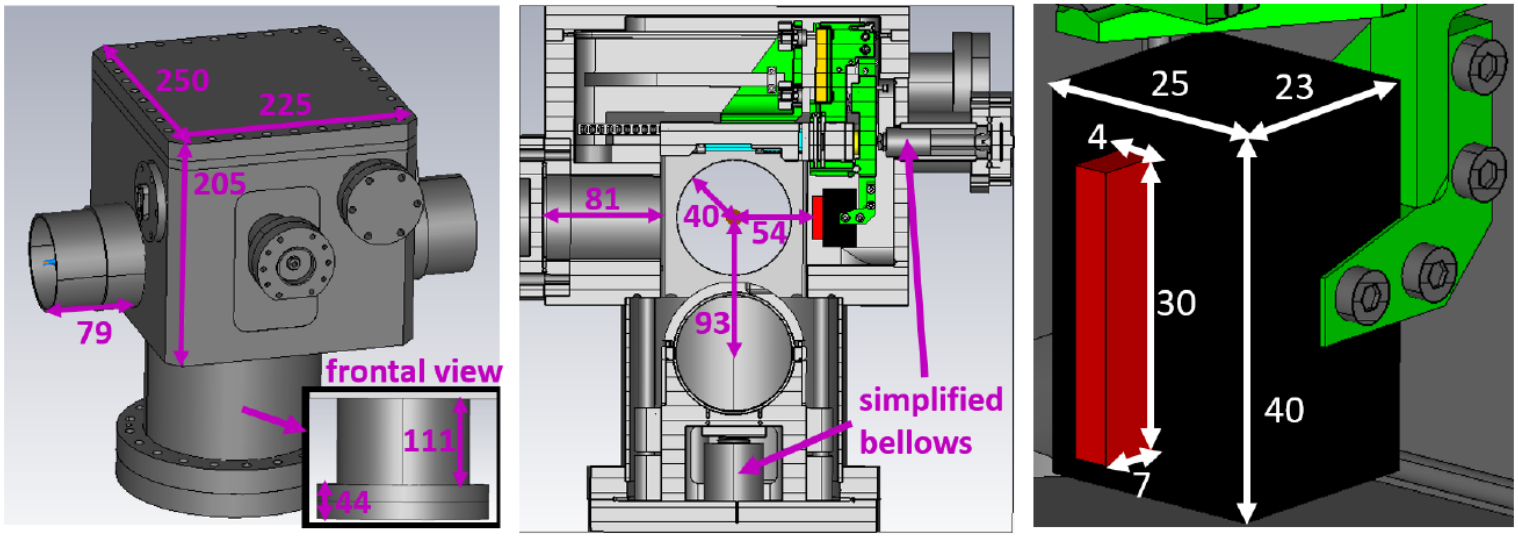

Material characterization

- Effort was spent to characterize the materials of the goniometer.

- The conductivity dispersion model has been used to characterize the mirror, crystal and piezo.

$$\epsilon'(f) \equiv \epsilon_r, \qquad \epsilon''(f) = \frac{\sigma_{el}}{2\pi\epsilon_0 f}$$

  - CST adopts by default this model to define the permittivity of dielectric materials.

- As for the crystal in silicon, the values of ε_r and σ_{el} were also taken from CST default values.
  - It's difficult to characterize the EM properties of the crystal, as shown later.

Zooms on some components made of different materials

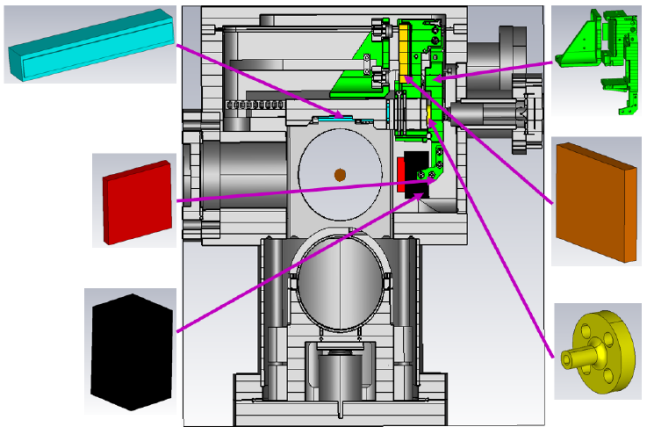

Crystal permittivity used in simulations

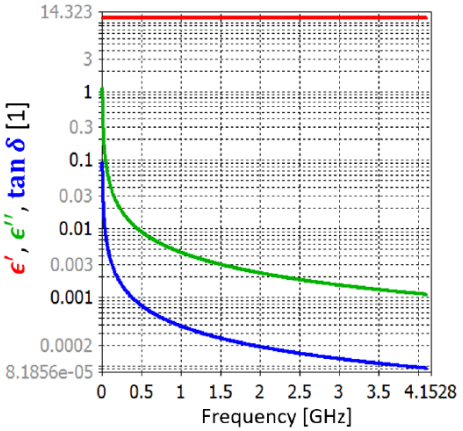

Characteristics of the materials

Component	Material	Type	ε_r [1]	σ_{el} [S/m]
External tank, replacement chamber, mechanical stage, …	stainless steel	conductor	1	1.3×10^6
Holder	titanium	conductor	1	5.8×10^5
Support for mirror and holder	aluminium	conductor	1	3.6×10^7
RF contact	gold	conductor	1	4.6×10^7
Mirror	glass	dielectric	7.5	1.0×10^{-11}
Crystal	silicon	dielectric	11.9	2.5×10^{-4}
Piezo	ceramic	dielectric	30	1.0×10^{-7}

Wakefield simulations with crystal & holder (1/2)

- δ_l denotes the distance between the beam-line and the crystal.
  - The replacement chamber is always retracted.

- δ_l = 54 mm: crystal in parking position, this configuration concerns HL-LHC proton beams and aims at assessing the need of the replacement chamber and the possibility of its removal from future goniometer models.

- δ_l = 14 mm: intermediate position used in RF measurements of the goniometer.

- δ_l = 8 mm, 2 mm: average settings for ion-beam operation at LHC injection and top energy, respectively.

- Simulations very time expensive (10-14 days) due to relatively long wake (500 m), relatively high number of mesh cells (35 M), presence of dielectrics with frequency dependent permittivity,…

Re Z from wakefield simulations (corresponding modes are marked by the same number)

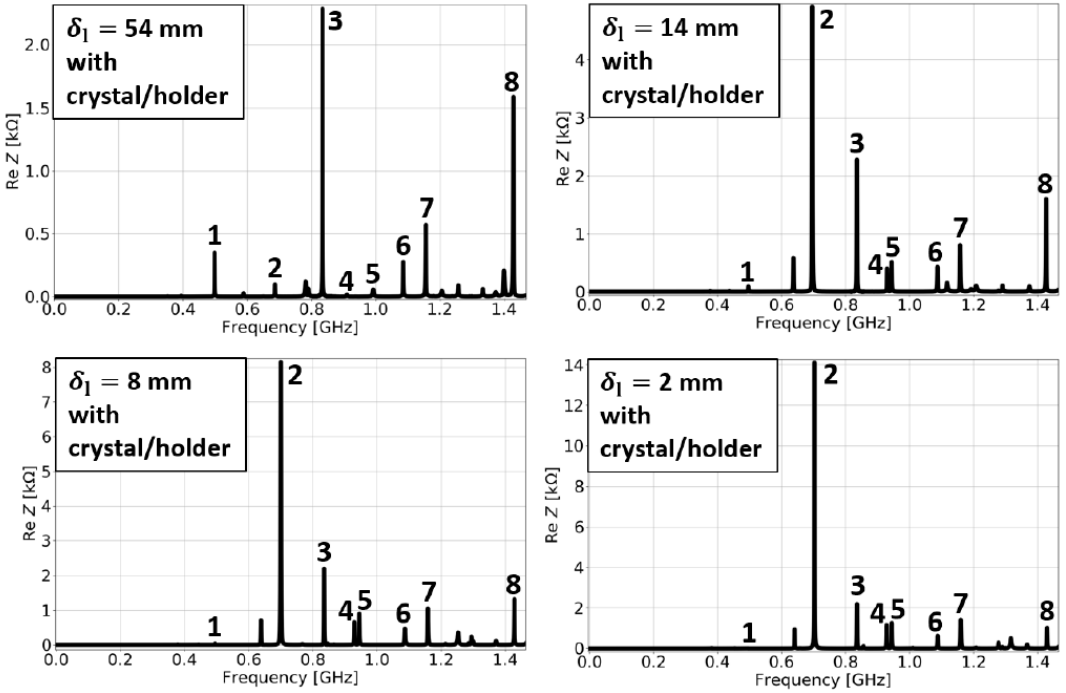

- Eight modes occur in all the four configurations.
  - Except for the resonance 3, all the modes significantly depend on δ_l.
  - For instance, R_s of mode 2 increases by more than factor 100 when the crystal approaches the beam line.

Wakefield simulations with crystal & holder (2/2)

- The dependencies $R_s(\delta_l)$ and $Q(\delta_l)$ vary for the different modes, for instance
  - Mode 1: R_s decreases and Q is constant as δ_l decreases.
  - Mode 2: R_s and Q increase as δ_l decreases.
  - Mode 3: R_s and Q are constant as δ_l decreases.

R_s and Q of the modes 1, 2 and 3 versus δ_l

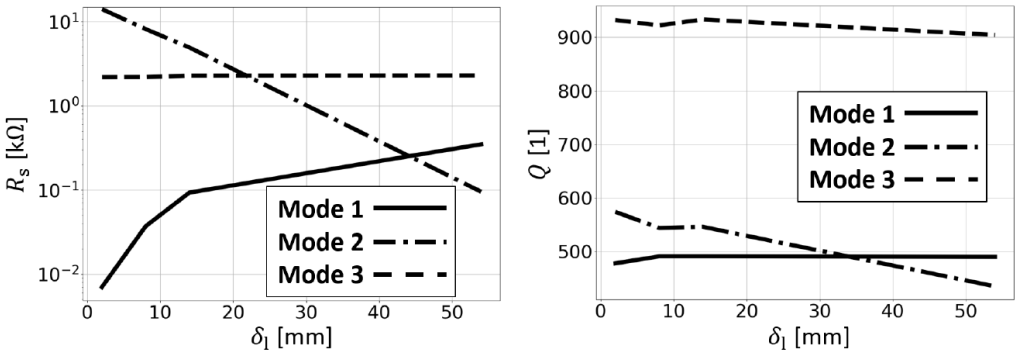

- E-field frequency monitors help to understand where the different modes are located, e.g.
  - Mode 1: is localized close to the replacement chamber when δ_l = 54 mm. For lower distance, it's close to crystal and holder.
  - Mode 2: is localized mostly close to the crystal and holder for each δ_l.
  - Mode 3: is largely localized close to the replacement chamber and is almost independent of the position of crystal and holder.

E-field monitors for the modes 1, 2 and 3 with varying δ_l

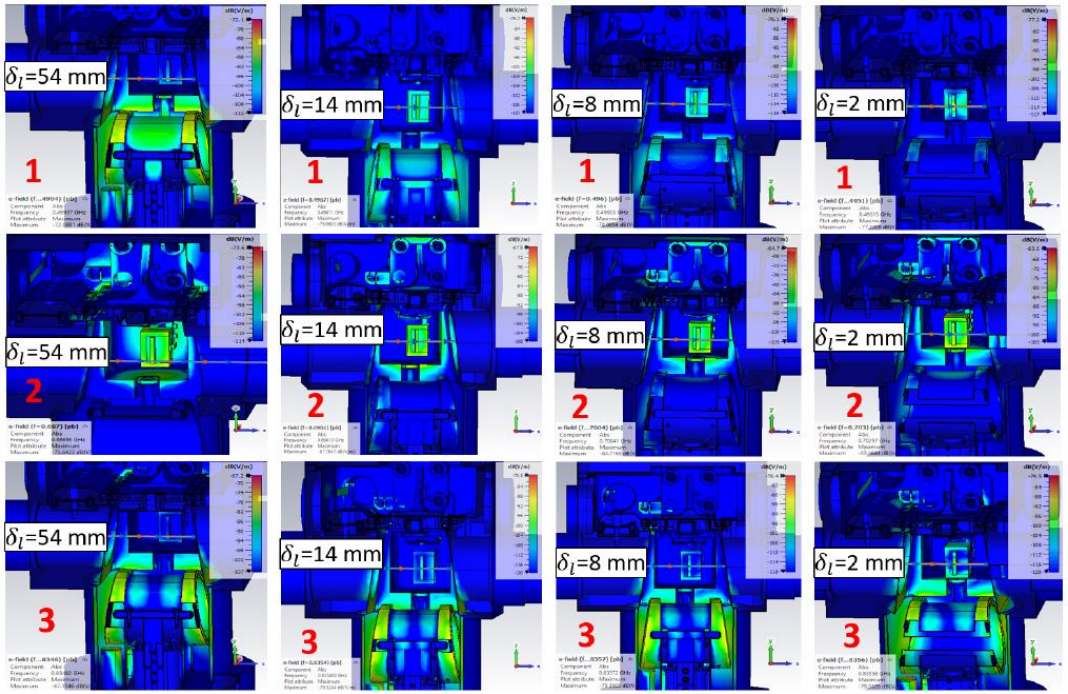

Wakefield simulations without crystal & holder (1/2)

- Although the model becomes unrealistic, simulations without crystal and holder were performed to
  - evaluate the impact of crystal and holder on the resonating modes;
  - benchmark measurements and simulations without the unknowns on the crystal properties.

- **δ_l = 54 mm:**
  - The modes 1, 3, 6, 7 and 8 are not substantially affected by the presence of crystal/holder.
    - The discrepancies in f_r and R_s are less than 1% and 10% respectively.
    - The low impact of crystal/holder is due to the fact that these modes are located in the bottom region of the external tank of the goniometer.
  - The modes 2 and 5 disappear when holder and crystal are removed.
    - Indeed these two modes resonate close to crystal and holder.

Re Z from wakefield simulations, with and without crystal/holder, δ_l = 54 mm and δ_l = 14 mm

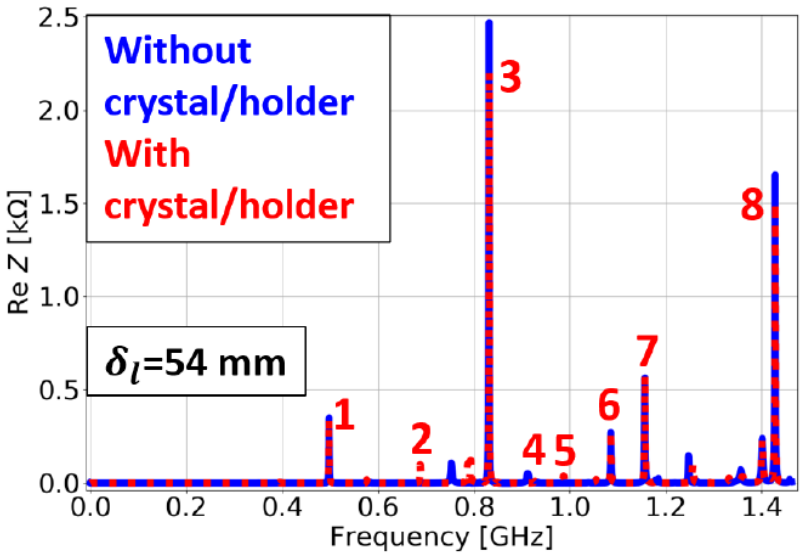

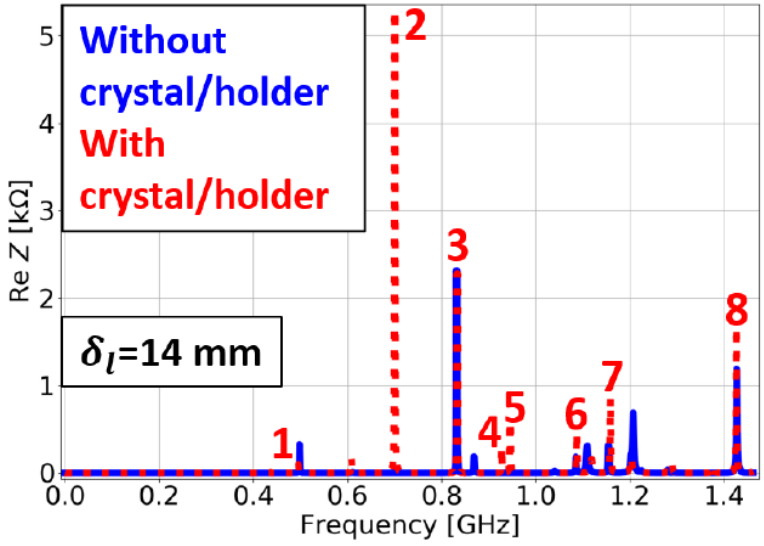

Wakefield simulations without crystal & holder (2/2)

- **δ_l = 14 mm:**
  - The modes 2, 4 and 5 disappear when crystal and holder are removed.
    - Additional simulations showed that these modes are essentially due to the holder, the crystal either doesn't have an influence or helps damping these modes lowering R_s and Q.
  - R_s of the modes 6 and 7 decreases by at least factor 2 when crystal and holder are removed.
  - R_s of the mode 1 increases by factor 3 when crystal and holder are removed.
  - The mode 3 isn't affected by the presence of crystal/holder.
    - Indeed it resonates in the bottom part of the external tank.

Re Z from wakefield simulations, with and without crystal/holder, δ_l = 54 mm and δ_l = 14 mm

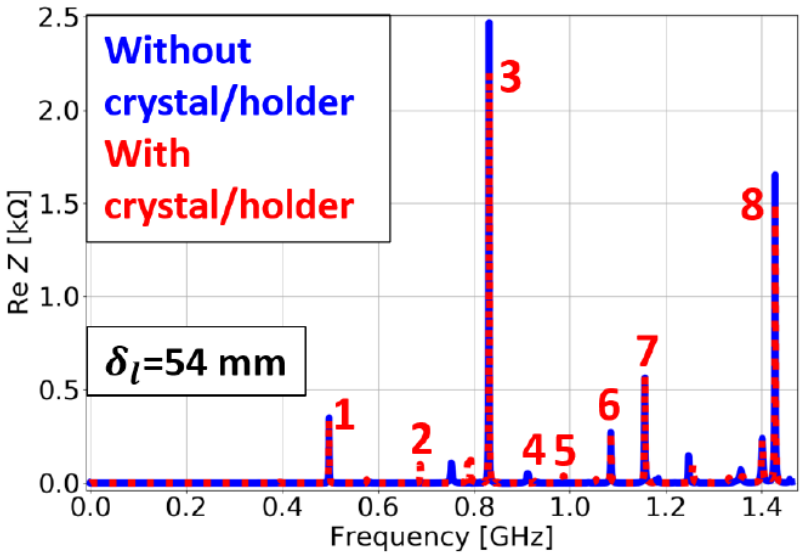

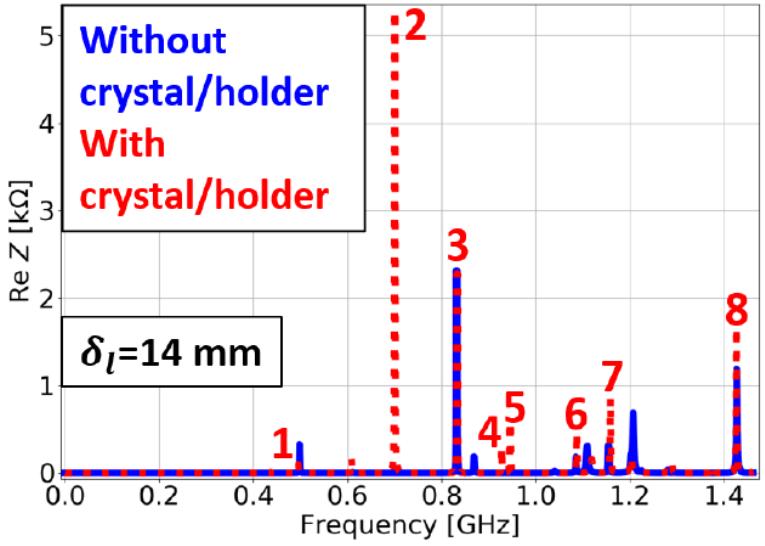

Benchmarks between wakefield and time-domain microwave simulations

- To validate wakefield simulations, time-domain microwave simulations were also performed.
  - A wire along the beam-line was used as source of EM fields.
    - This method resembles the one used in RF wire measurements of the goniometer presented later.

- In general, we see good agreement in f_r between corresponding modes.

- Almost always, resonances with higher R_s have lower $|S_{21}|$ minimum-values.

- This indicates that wire-measurements should allow identifying the modes of the goniometer.

$|S_{21}|$ and Re Z from wakefield and microwave simulations, δ_l=14 mm, without and with crystal/holder

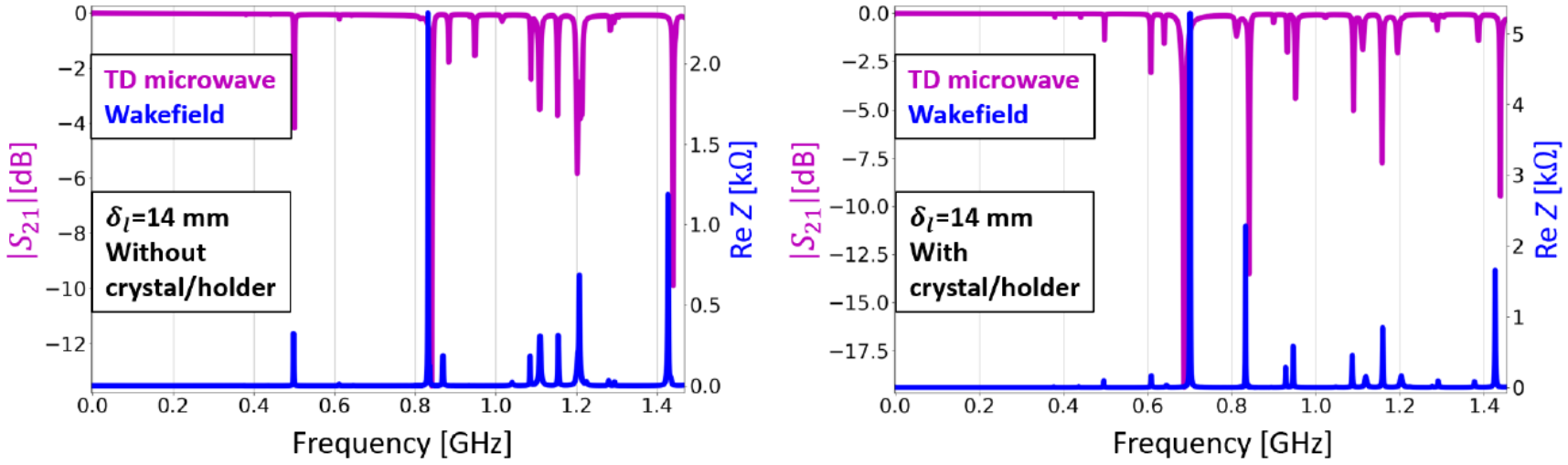

Modes sensitivity to crystal complex permittivity (1/3)

- RF cavity-perturbation measurements were performed in 2017 in order to characterize the permittivity of the crystal in the range 2 GHz – 4 GHz.
  - Measurements performed by measuring the TE_{10} modes of an empty rectangular cavity connected to a VNA and by measuring the same cavity with a sample of crystal inside.

- The permittivity was estimated by evaluating the changes in f_r and Q of the different modes when the crystal was inserted into the cavity

$$\epsilon'(f_{r,e}) = 1 + \frac{V_c}{4V_s}\left(\frac{f_{r,e}^2}{f_{r,p}^2} - 1\right) \qquad \epsilon''(f_{r,e}) = \frac{V_c}{4V_s}\frac{f_{r,e}^2}{f_{r,p}^2}\left(\frac{1}{Q_p} - \frac{1}{Q_e}\right)$$

e: absence of crystal
p: presence of crystal
V_c: volume of the cavity
V_s: volume of the crystal

- The obtained permittivity values showed a significant dependence on the crystal position with respect to the E-field lines of the TE_{10} modes.

Left (right): the circles are the measurements results when the crystal is in the transversal (longitudinal) position with respect to the E-field lines of the TE_{10} modes.

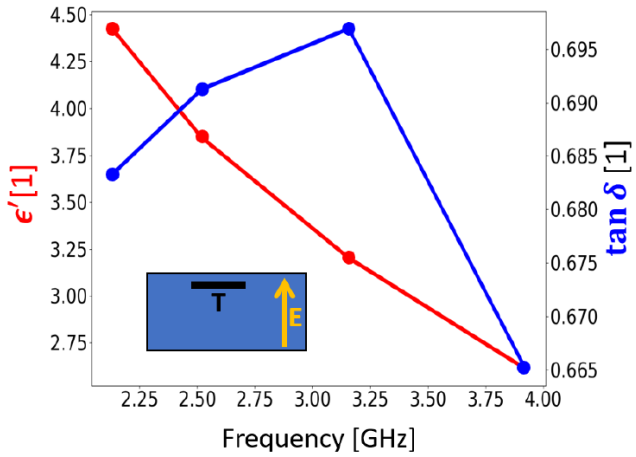

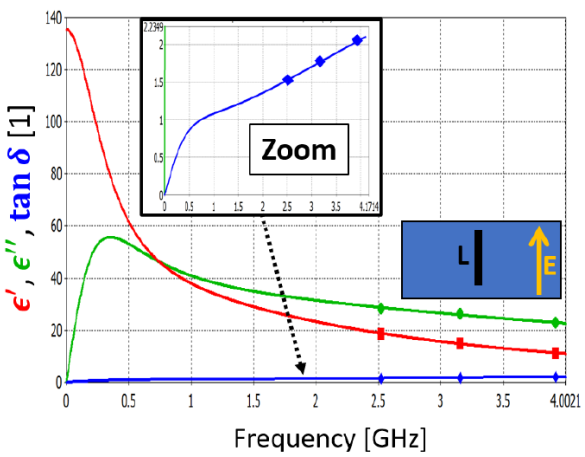

Modes sensitivity to crystal complex permittivity (2/3)

- We were interested in evaluating the effect of relatively large loss-tangent values on the modes resonating inside the goniometer.
  - The permittivity measurements with the crystal in longitudinal position were taken into account.

- It was necessary to perform an extrapolation of these measurements to obtain values below 1.5 GHz.
  - This was done using CST, which allows fitting the measured permittivity values with a superposition of dielectric dispersion models of first and second order

$$\epsilon(\omega) = \epsilon_\infty + \sum_{n=1}^{N} \frac{\beta_{0,n}}{\alpha_{0,n} + j\omega} + \sum_{n=1}^{M} \frac{\gamma_{0,n} + j\omega\gamma_{1,n}}{\delta_{0,n} + j\omega\delta_{1,n} - \omega^2}$$

ε_∞: high-frequency limit
$\alpha_{0,n}$, $\beta_{0,n}$: parameters of the 1st order models
$\gamma_{0,n}$, $\gamma_{1,n}$, $\delta_{0,n}$, $\delta_{1,n}$: parameters of the 2nd order models

- The permittivity which provided the smallest rms error when compared with the measured data was the sum of two first-order dispersion models

$$\epsilon(\omega) = \epsilon_\infty + \frac{\beta_{0,1}}{\alpha_{0,1} + j\omega} + \frac{\beta_{0,2}}{\alpha_{0,2} + j\omega}$$

- This permittivity from fit differs significantly from the CST dispersion model used in simulations.
  - E.g. tan δ at 700 MHz is lower by factor 3700 in the conductivity model.

Right: the measured permittivity values (circles) are fitted with a sum of two first-order dispersion models

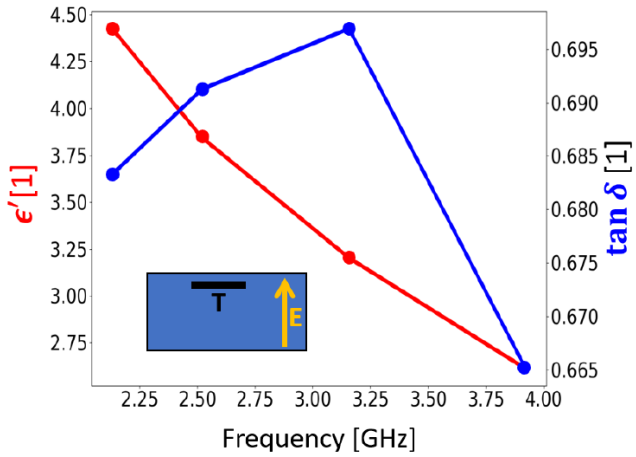

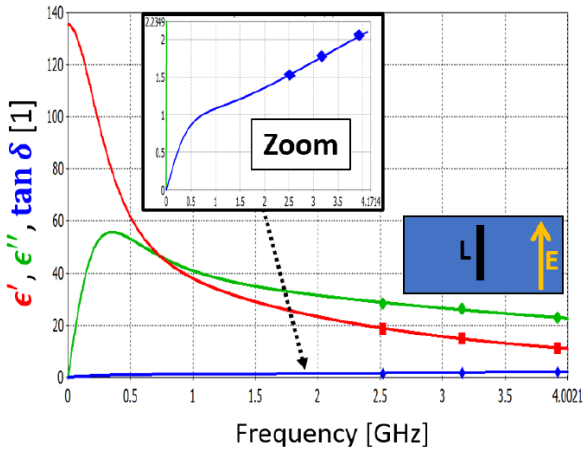

Modes sensitivity to crystal complex permittivity (3/3)

- To understand how different crystal permittivities affect the modes of the goniometer, wakefield simulations were performed using also the permittivity from the fit.

- The comparison is good, with the largest differences concerning the R_s and Q of the mode 2 at 700 MHz.
  - When tanδ is large, the crystal damps the mode at 700 MHz due to the holder.
    - Indeed large tanδ values lead to higher values of power absorbed by the crystal, and this helps damping the mode.

- Due to the uncertainties on the crystal properties, we used the conductivity model in simulations.
  - Additional measurements and studies are needed to better characterize the crystal properties.
    - The possibility that the crystal is anisotropic should be investigated.

Re Z from wakefield simulations, permittivity from conductivity model or from measurements fit

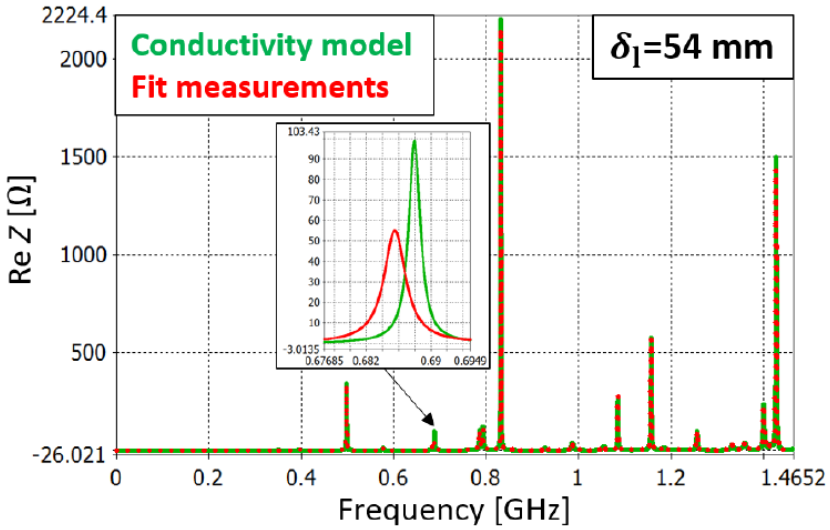

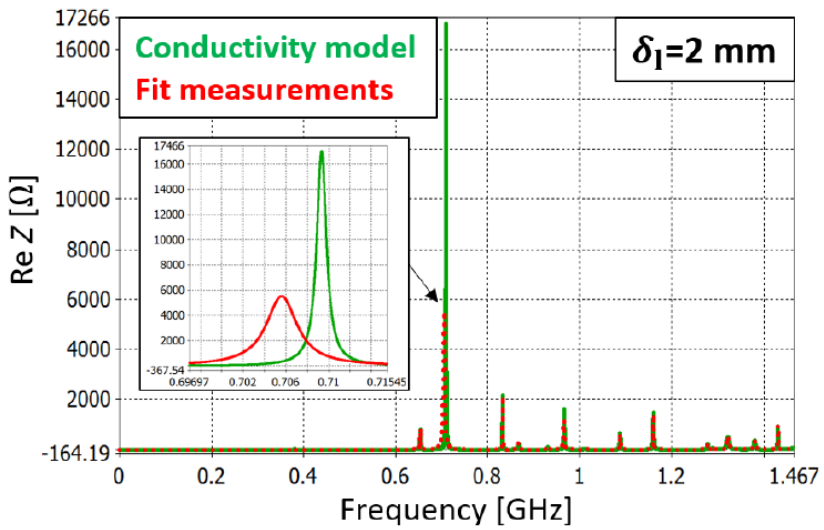

Contents

Studied LHC beams (1/2)

- Five types of LHC beams are considered for the evaluation of the power losses in the goniometer.
- For each beam, the line-density at LHC top-energy is reproduced numerically taking into account the specific beam filling-pattern and the expected single-bunch charge, longitudinal shape and length.
- According to operational experience and future expectations, the longitudinal bunch-profile at LHC top energy is well described by a Tsallis q-Gaussian distribution at the beginning of a beam fill, while at the end of it the profile tends to be Gaussian.
- For power-loss estimations, we assume that
  - the bunch-profiles in a given beam are described by the same distribution, Gaussian or q-Gaussian;
  - the bunch-profiles in a given beam have the same bunch length, equal to the measured or estimated average value.

Main parameters of the LHC beams considered for the evaluation of power-losses

Type of LHC beam	Type of particle	Year	Number of bunches	Bunch spacing [ns]	Intensity per bunch [ppb]	Beam charge [e]	Average bunch length (4 σ) [ns]
Fill5979	proton	2017	2556	25	1.1×10^{11}	2.8×10^{14}	1.08
HL2760b	proton	HL	2760	25	2.3×10^{11}	6.3×10^{14}	1.20
8b4eHL	proton	HL	1972	25	2.3×10^{11}	4.5×10^{14}	1.20
Fill7467	$^{208}_{82}Pb$	2018	733	75	2.1×10^{8}	1.3×10^{13}	1.10
IonHL	$^{208}_{82}Pb$	HL	1240	50	1.8×10^{8}	1.8×10^{13}	1.10

Studied LHC beams (2/2)

- Examples of numerically reconstructed line densities of the proton Fill5979 and 8b4eHL beams.
- In these examples, the bunches have a Gaussian distribution.
- The beam power-spectra become relatively small after 1.5 GHz.
- The peculiar filling-pattern of the 8b4eHL beam is used for electron-cloud mitigation and produces side-bands around the main power-spectrum lines.
- The beam-spectra are directly used in the computation of power losses.

Reconstructed line-density (top left) and power-spectrum (top right) of the Fill5979-beam at LHC top-energy. Consecutive zooms on the line density are shown (bottom).

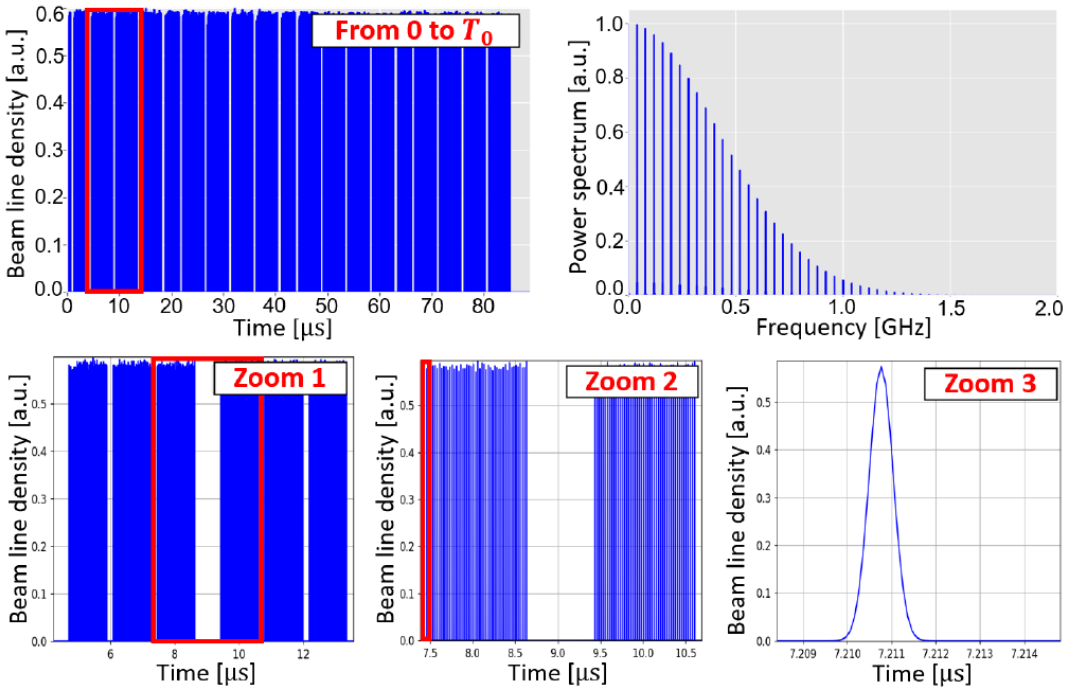

Reconstructed line-density (left), zoom (middle) and power-spectrum (right) of the 8b4eHL-beam at LHC top-energy.

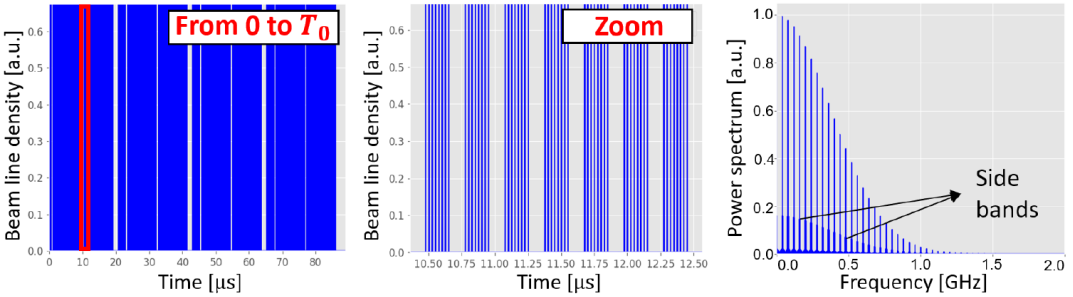

Method to evaluate power losses

- Given a certain longitudinal impedance Z and a normalized beam power-spectrum Λ, the total power dissipated inside the goniometer is computed as

$$P = f_0^2 q^2 N_{beam}^2 \sum_{p=-\infty}^{+\infty} |\Lambda(p f_0)|^2 \mathrm{Re}[Z(p f_0)]$$

- In fact this formula was not used directly, since the obtained results could be significantly affected by the uncertainties on Λ and Z.
  - Λ can change with time during beam motion, even at constant energy, due to dipole and/or higher-order oscillations.
  - Z derives from simulation results, where potential numerical inaccuracies and unknowns on the model (e.g. crystal) could be present.
    - In particular, the computed resonant frequencies don't necessarily coincide with those of the real device, and this can affect the power-loss estimations depending if the resonant frequency of a mode coincides with a line of the beam-spectrum.

- For each beam, a perturbative analysis on Z was performed.
  - The impedance was shifted within plus or minus 20 MHz on 200 frequency points, the corresponding power-losses were computed with the formula above, and finally the average and maximum of these obtained values were considered.
  - This analysis allows to take into account, at least in part, the variations in f_r of the modes.

Protons: beam-crystal distance of 54 mm

- Although the baseline scenario for protons is to have the replacement chamber parked in, we evaluated the power-losses for protons when the chamber is parked out and δ_l = 54 mm.

- The power-losses depend largely on N_{beam}, equal to 2.81×10^{14} ppb for Fill5979, 6.35×10^{14} ppb for HL2760b, 4.54×10^{14} ppb for 8b4eHL.

- q-Gaussian profiles lead to an increase in dissipated power by roughly factor 1.5.

Power losses assuming that the profiles are Gaussian or q-Gaussian (values in parentheses)

LHC proton beam	δ_l [mm]	Average power [W]	Maximum power [W]
Fill5979	54	23.5 (34.6)	195.3 (305.9)
HL2760b	54	76.8 (111.0)	595.1 (981.5)
8b4eHL	54	52.6 (75.3)	305.1 (501.6)

- The average and maximum power-loss densities show that, for each proton beam,
  - the two major contributions come from the modes 1 and 3, at 500 MHz and 835 MHz respectively.
    - There modes, with high R_s and Q, are located in the bottom region of the external tank.
  - the modes between 1 and 3 (including mode 2, which depends on crystal and holder) provide non-negligible contributions.
  - the modes above 900 MHz lead to relatively small contributions due to the beam-spectrum decay.

Power-loss densities assuming Gaussian profiles. Average (left) and maximum (right) values from the perturbative analysis

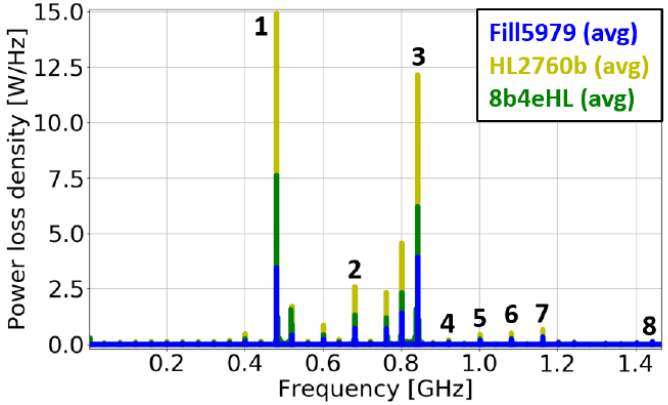

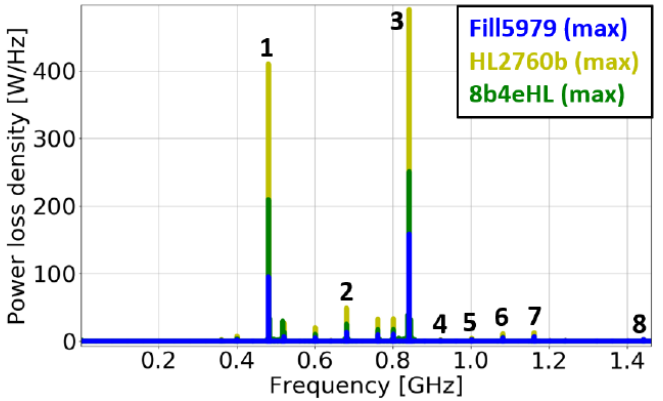

Ions: beam-crystal distance of 8 mm and 2 mm

- The goniometer is supposed to be operational for ion beams with average δ_l of 8 mm and 2 mm at injection and top energy respectively.
- The power-losses are higher at top energy than at injection.
  - This is mainly due to the larger R_s of the mode 2 when δ_l = 2 mm.
- q-Gaussian profiles lead to an increase in dissipated power by roughly factor 1.5.
- The power-losses for protons are in general higher than the ones for ions by one or two order of magnitudes.
  - This is largely explained by the lower number of charges and bunches in the ion beams: N_{beam} is 1.26×10^{13} protons for Fill7467, 1.83×10^{13} protons for IonHL.
- The major contributions to the power-losses come from the mode 2.
- The modes above 1 GHz lead to small contributions to power losses.

Power losses assuming that the profiles are Gaussian or q-Gaussian (values in parentheses)

LHC ion beam	δ_l [mm]	Average power [W]	Maximum power [W]
Fill7467	8	0.62 (0.92)	2.63 (3.65)
	2	1.02 (1.41)	4.23 (6.01)
IonHL	8	0.78 (1.28)	5.53 (7.71)
	2	1.10 (1.51)	8.84 (12.53)

Power-loss densities for the Fill7467 beam assuming Gaussian profiles. Average (left) and maximum (right) values, at injection (top) and top-energy (bottom)

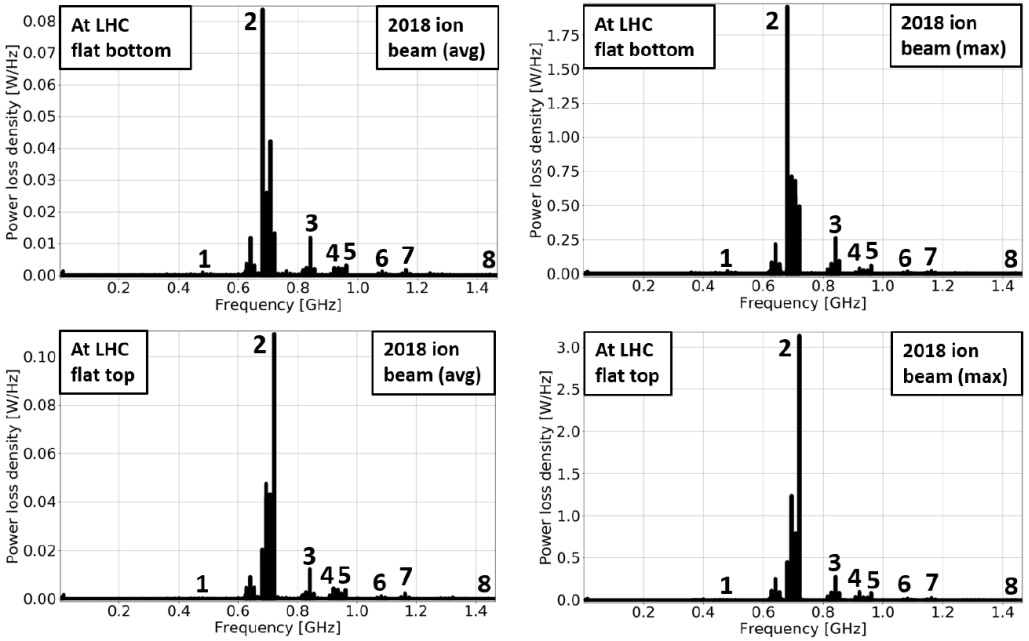

Heat load localization

- In order to assess the heat-load localization, H-field frequency monitors were added in simulation.
  - Mode 1:
    - When δ_l = 54 mm, this mode dissipates power in the bottom region of the external tank.
    - When δ_l = 2 mm, the heat load is localized close to the holder and crystal.
  - Mode 2: independent of δ_l, the power is largely deposited on the crystal, holder, aluminum support and mechanical stage. In particular, the H-field is larger close to the holder support.
  - Mode 3: independent of δ_l, this mode dissipates power in the bottom region of the external tank. The H-field is relatively large also close to the crystal and holder-support when δ_l = 2 mm.

- In good approximation, the E-field and H-field of a given mode have larger magnitudes in the proximity of the same goniometer components.
  - E.g. the EM fields of the mode 2 are localized close to the holder.

H-fields for the modes 1, 2 and 3, δ_l=54 mm (top) and δ_l=2 mm (bottom)

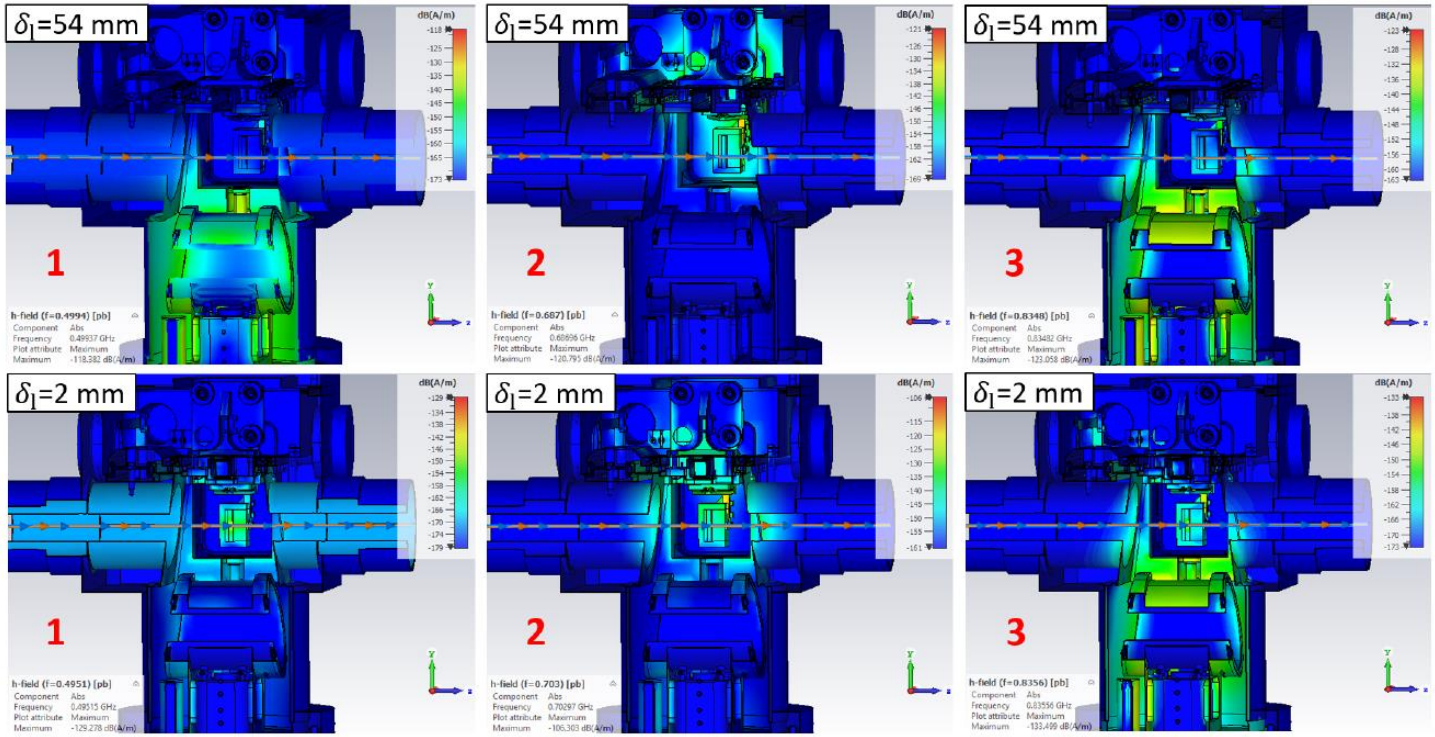

Contents

RF-measurements setups (1/2)

- In addition to simulations, RF wire and probe measurements of the goniometer were performed in 2019 to characterize the longitudinal impedance of the device.

- In measurements, δ_l was either 54 mm or 14 mm, with or without the crystal/holder assembly.
  - Lower δ_l weren't considered to avoid accidental collisions between crystal and wire.

- In wire-measurements, a copper-beryllium wire with radius r = 0.25 mm was stretched along the device and the transmission parameter S_{21}^{DUT} was measured.

- Then, S_{21}^{DUT} was compared to the reference S_{21}^{REF}, which was the transmission of the wire/beam-pipe ensemble, i.e. a TEM coaxial line with inner radius r and outer radius R = 40 mm.

- The longitudinal impedance was obtained using the log-formula

$$Z_{log} = -2Z_{\mathrm{C}} \ln \frac{S_{21}^{\mathrm{DUT}}}{S_{21}^{\mathrm{REF}}}$$

- The line-impedance of the TEM coaxial line was evaluated as

$$Z_{\mathrm{C}} = \frac{Z_0}{2\pi} \ln \frac{R}{r} \approx 300\,\Omega$$

Setups of the 2019 RF wire (left) and probe (right) measurements of the goniometer

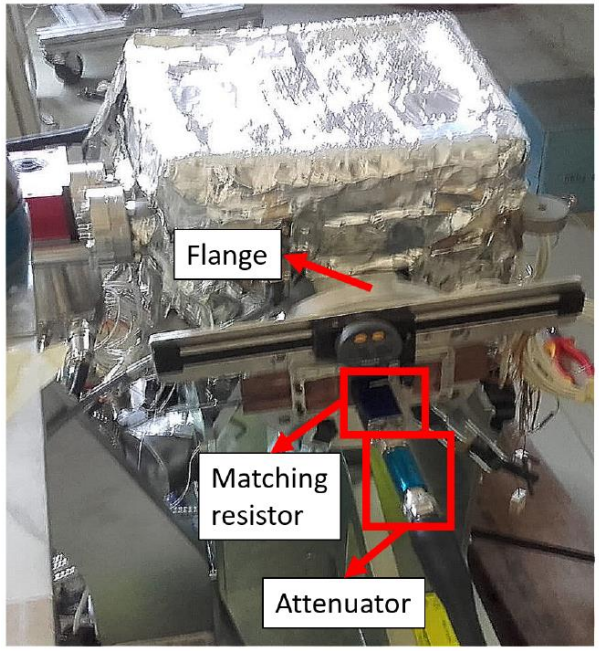

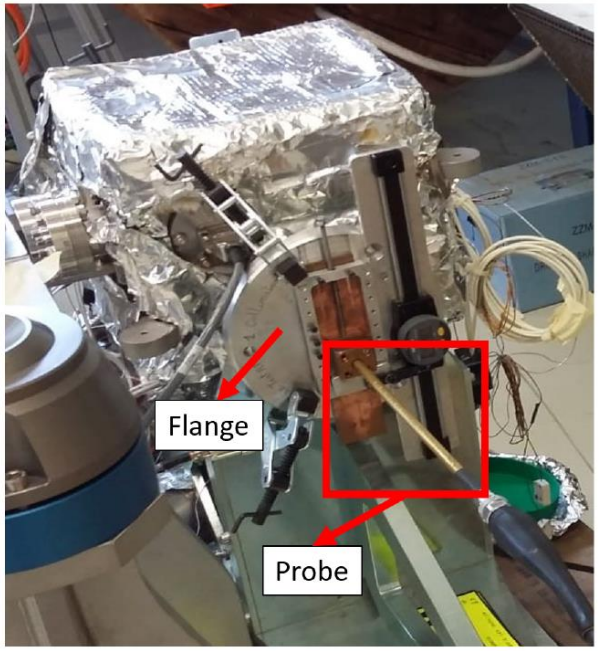

RF-measurements setups (2/2)

- Since the VNA had an internal impedance of 50 Ω, two resistors of approximately 250 Ω were inserted between the VNA coaxial cables and the wire in order to match the goniometer and VNA impedances.
- 10 dB attenuators were inserted close to the resistor in order to reduce the residual signal-reflections due to the inaccuracies of the matching.
- The wire method isn't well suited to characterize high-Q resonances.
  - The presence of the wire detunes f_r and decreases Q.
- Therefore, probe measurements were also performed inserting probes into the goniometer.
- The f_r and Q of the modes were evaluated examining the measured S_{21}.
- The reflection parameters S_{11} and S_{22} were analysed to verify that the probes were weakly coupled.
  - In some cases this condition could be satisfied only by changing the probe type and the length of penetration inside the device.

Setups of the 2019 RF wire (left) and probe (right) measurements of the goniometer

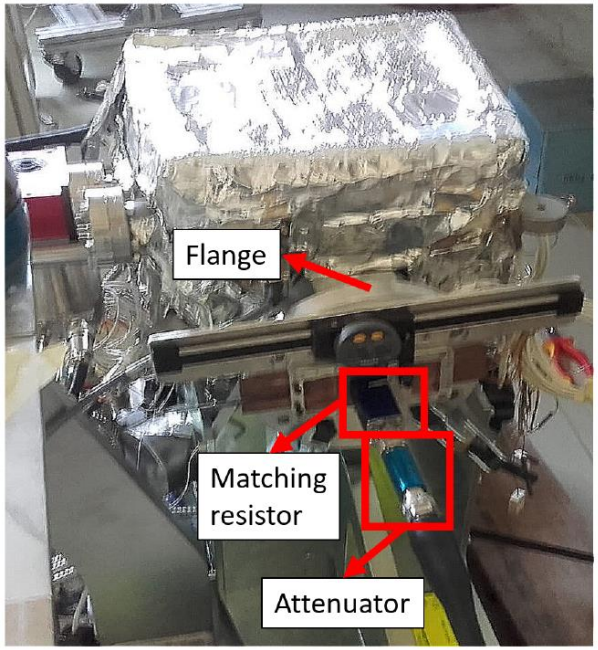

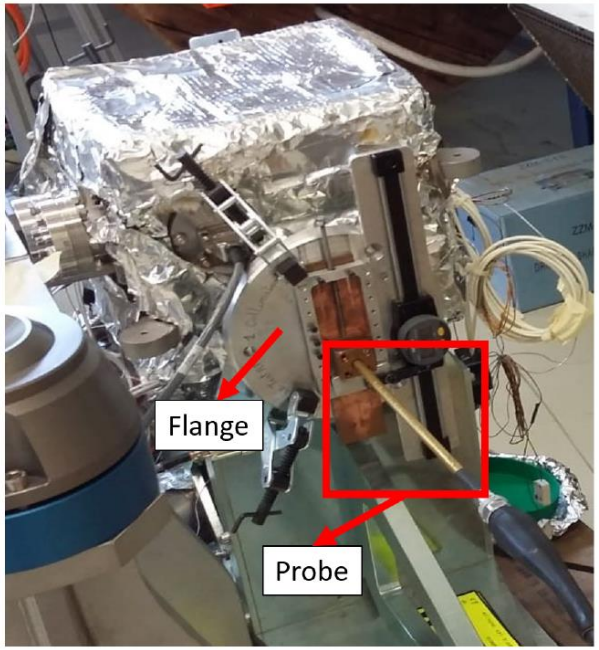

Wire-measurements results (1/2)

- The non-perfect match between VNA and goniometer led to signal reflections, which in turn produced baseline-oscillations in the measured transmission parameters.

- These oscillations were eliminated reconstructing the baseline in correspondence of the modes by performing polynomial fits and then subtracting this baseline from the measured signal.

- The modes marked by numbers are visible in all the four measured goniometer setups.

- The mode 3 has the lowest $|S_{21}|$ for all the four cases.
  - The corresponding minima are lower when crystal and holder are removed.

Left: example of measured $|S_{21}|$ with fits for baseline reconstruction
Right: difference between $|S_{21}|$ and the reconstructed baseline

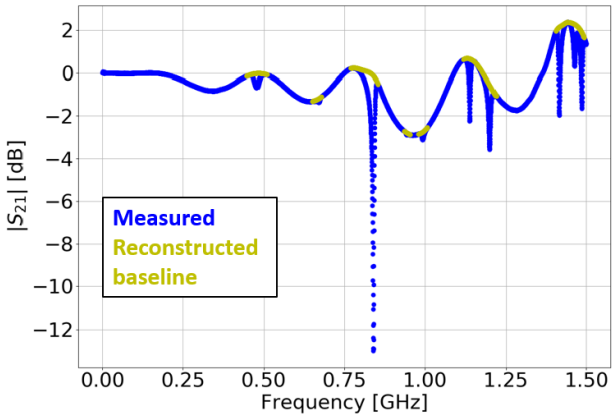

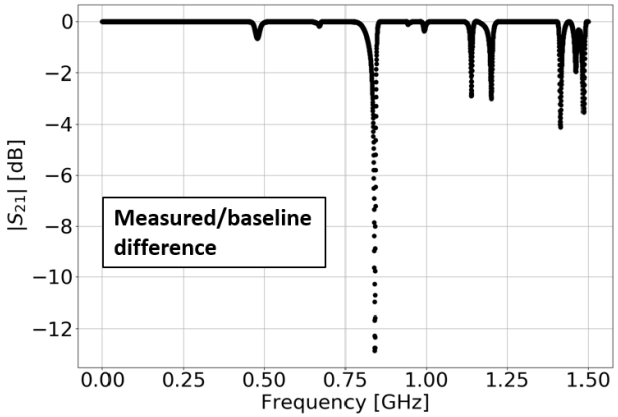

$|S_{21}|$ from wire-measurements after having removed the baseline oscillations, δ_l=54 mm (left) and δ_l=14 mm (right)

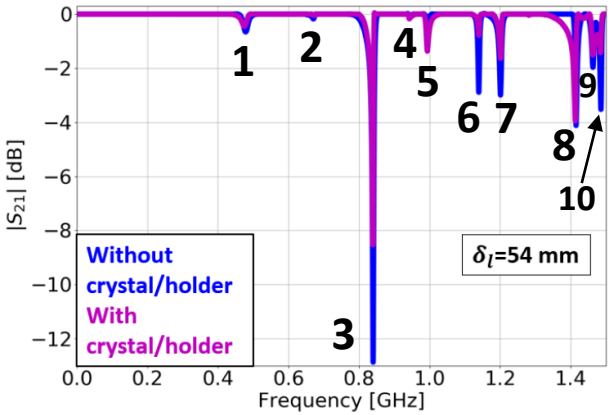

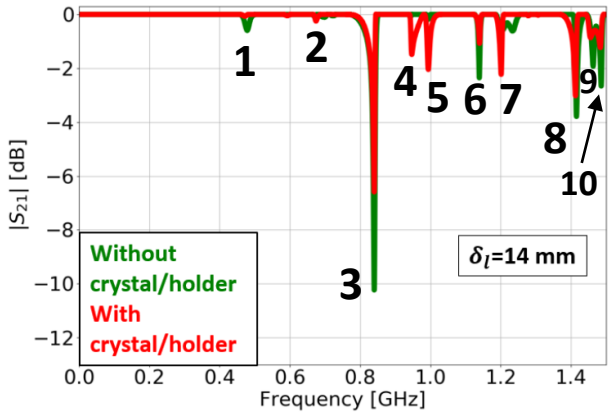

Wire-measurements results (2/2)

- The log-formula was used to convert the transmission parameters into impedances.

- Although affected by the presence of the wire inside the goniometer, R_s, f_r and Q of the different modes can be evaluated and compared, for instance
  - **Modes 1 and 3:**
    - R_s decreases adding crystal and holder, regardless of δ_l.
    - R_s decreases when δ_l changes from 54 mm to 14 mm for a given configuration (with crystal/holder or without).
  - **Mode 2:**
    - The smallest and largest R_s occur when the crystal is parked out and in respectively.

Re Z obtained applying the log-formula to the corresponding $|S_{21}|$, δ_l = 54 mm (left) and δ_l = 14 mm (right). Zooms on some modes are also shown.

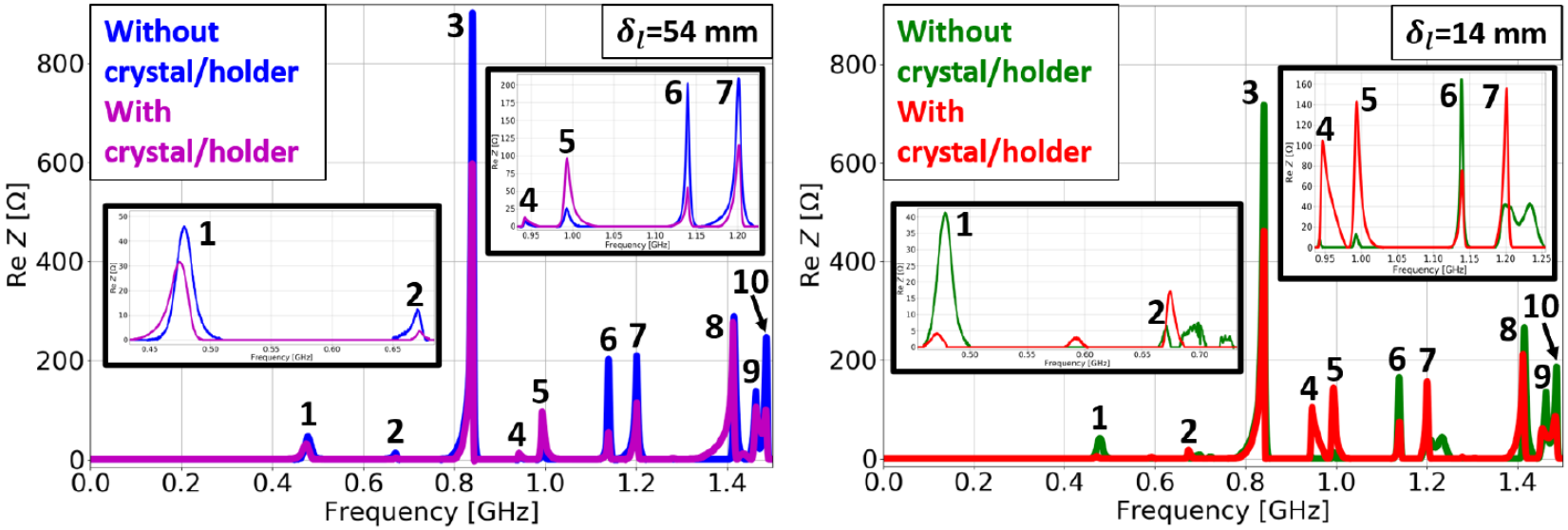

Probe-measurements versus wire-measurements

f_r and Q of the modes found in probe measurements. For each mode, the Q factor and the number of the corresponding mode from wire-measurements is between parentheses.

		Q (δ_l=54 mm)		Q (δ_l=14 mm)	
	f_r [MHz]	Without holder/crystal	With holder/crystal	Without holder/crystal	With holder/crystal
→	480, 483, 481, 479	28 (31, mode 1)	56 (28, mode 1)	40 (34, mode 1)	58 (41, mode 1)
	672, 687, 672, 690	136 (91, mode 2)	8 (110, mode 2)	123 (132, mode 2)	n.d. (88, mode 2)
→	838	388 (169, mode 3)	465 (180, mode 3)	220 (138, mode 3)	219 (138, mode 3)
→	941	267 (196, mode 4)		341 (314, mode 4)	
→	993	140 (143, mode 5)		135 (171, mode 5)	
→	1140	279 (242, mode 6)	215 (260, mode 6)	215 (251, mode 6)	256 (230, mode 6)
	1200	230 (165, mode 7)	249 (181, mode 7)	120 (n.d., mode 7)	258 (185, mode 7)
→	1407	267 (240, mode 8)		214 (229, mode 8)	

n.d.: Q couldn't be determined since the bandwidth was not defined.

- Corresponding modes from probe and wire measurements differ in f_r by less than 3%.
- All the modes found with the probe were also measured with the wire.
- The modes 1, 3 and 6 are visible in probe and wire measurements, regardless of the goniometer setup.
- On the contrary, the modes 4, 5, 8 occur in probe measurements only in the absence of crystal and holder.
- Some discrepancies in Q are significant, possibly due to the fact that probe and wire affect in different ways the modes parameters or that in some cases, narrow-band modes from wire measurements couldn't be sufficiently sampled with the VNA.

Contents

Microwave simulations versus wire measurements

- Time-domain microwave simulations were compared with wire measurements.
  - As shown earlier, all the modes found with the probe were also found with the wire, therefore these comparisons take into account all the measured resonances.

- Examples of agreements:
  - The measured modes 1, 3, 8 have correspondences in f_r with modes found in simulations.
  - Correspondences also occur for the modes 2 and 5 when holder and crystal are present and δ_l = 54 mm.

- Disagreements:
  - In some cases correspondences in f_r couldn't easily be made.
  - In general, the minima of $|S_{21}|$ are smaller in simulations than in measurements.
  - The largest discrepancy occurs for the mode 2 when holder and crystal are present and δ_l = 14 mm.

$|S_{21}|$ from microwave simulations (red) and wire-measurements (blue). Zooms on some modes are also shown.

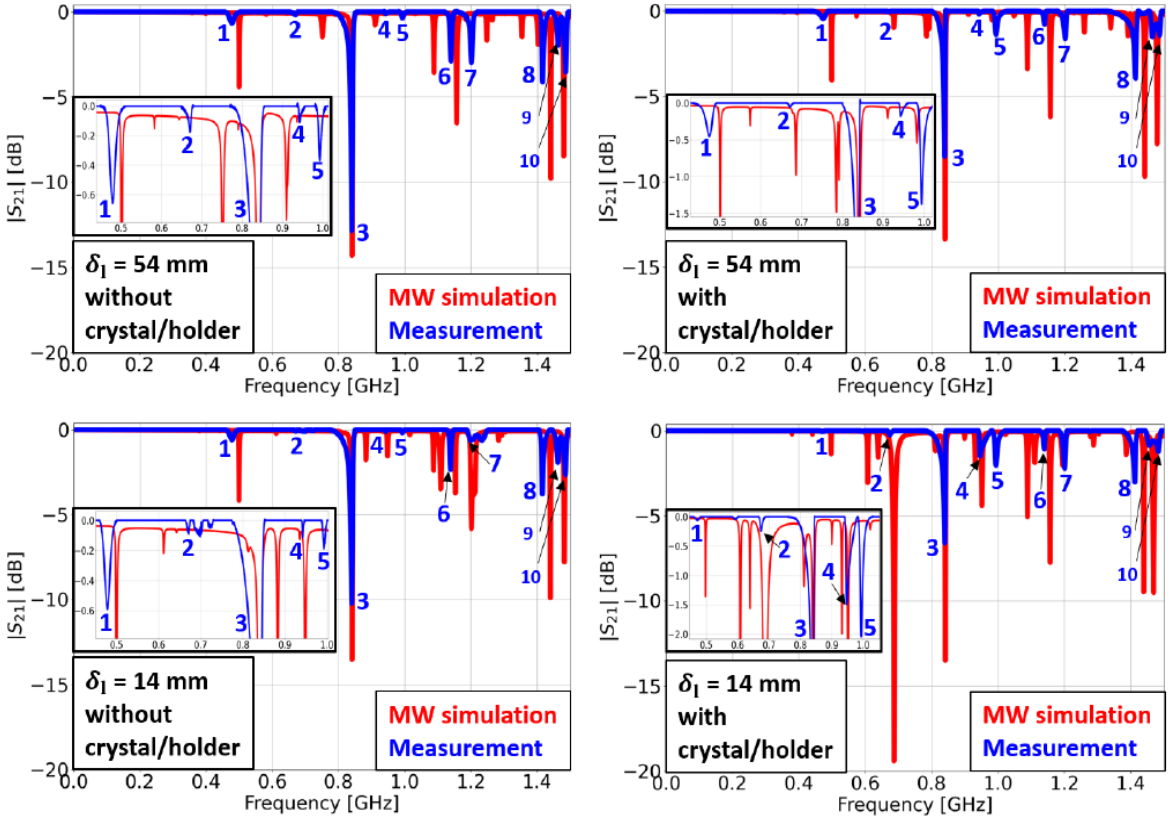

Wakefield simulations versus wire measurements

- Impedances from wakefield simulations were compared with impedances obtained from wire measurements applying the log-formula to the transmission parameters.

- The agreements in f_r correspond largely to the ones found earlier between microwave simulations and wire measurements.
  - For instance, the measured modes 1, 3, 8 have correspondences in f_r with modes found in wakefield simulations.

- The disagreements correspond to the ones between microwave simulations and wire measurements.
  - For instance, Q and R_s for pairs of corresponding modes are generally larger in simulations than in measurements.
  - The largest discrepancy occurs for the mode 2 when holder and crystal are present and δ_l = 14 mm.

Re Z from wakefield simulations (red) and wire-measurements (blue). Zooms on some modes are also shown.

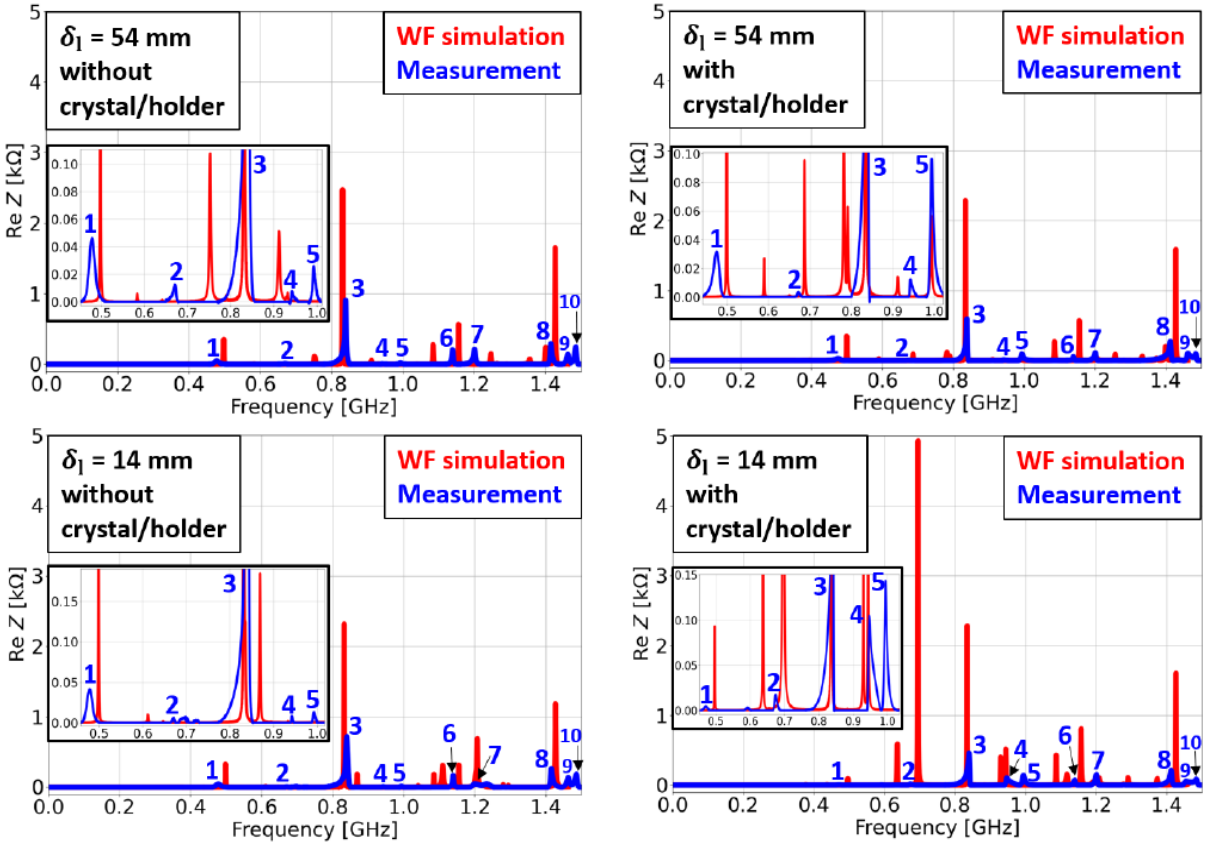

Power-losses using impedance from measurements

- The impedance from measurements when holder and crystal are present and δ_l = 54 mm was used to determine the power losses for the three proton beams described earlier.

Power losses assuming that the profiles are Gaussian or q-Gaussian (values in parentheses). The impedance used is obtained from wire measurements.

LHC proton beam	δ_l [mm]	Average power [W]	Maximum power [W]
Fill5979	54	28.93 (36.26)	76.42 (103.21)
HL2760b	54	108.13 (129.73)	350.11 (372.05)
8b4eHL	54	69.96 (86.94)	192.98 (209.47)

- Comparing these power losses with those obtained earlier using the impedance from simulation, we note that
  - the estimated average-power values are up to 50% larger in measurements than in simulation;
  - the estimated maximum-power values are up to 65% lower in measurements than in simulation.

- Qualitatively, these differences in power losses are due to the larger R_s and Q values of the simulated modes which couple less with the beam-spectrum lines on average, although they lead to large power losses when their resonant frequencies coincide with the beam-spectrum frequencies.

- Considering that the resonances found with the probe are confirmed by the wire method, results from wire measurements can confirm that no important measured high-Q mode is missing in simulations, as the comparisons shown earlier indicate.

Conclusions

- The LHC goniometers are crystal primary collimators which will be used in the HL-LHC era.
  - The goniometers will be used during the ion-beam runs starting in 2022.

- The longitudinal impedance of the device was characterized through measurements and simulations.

- Simulations took into account different configurations of the goniometer: setups with the replacement chamber in parking position and with the crystal at different distances from the beam-line.

- Effort was spent to characterize in simulation the materials of the device components.
  - As concerns the crystal, measured permittivity values were compared with standard ones, and the effect of these permittivities on the modes was evaluated.
    - Only the mode at 700 MHz was significantly affected by the permittivity.

- Dedicated RF wire and probe measurements were performed on one LHC goniometer.
  - The frequencies of all relevant modes found with the probe were also measured with the wire.

- Some discrepancies in mode parameters were observed between measurements and simulations,
  - However results confirmed that no important measured high-Q mode is missing in simulations.

- The longitudinal impedances obtained from simulations and realistic LHC beam parameters were used to provide power loss values for ion and proton beams in the current and HL-LHC scenarios.
  - Power loss densities were also provided, highlighting the modes and the device components